Appl. Phys. B 86, 511–514 (2007)
DOI: 10.1007/s00340-006-2501-x

Applied Physics B
Lasers and Optics

V.N. BURAKEVICH[1]
V.A. LISINETSKII[1,✉]
A.S. GRABTCHIKOV[1]
A.A. DEMIDOVICH[2]
V.A. ORLOVICH[1]
V.N. MATROSOV[3]

Diode-pumped continuous-wave Nd:YVO_4 laser with self-frequency Raman conversion

[1] B.I. Stepanov Institute of Physics, National Academy of Sciences of Belarus, Nezalezhnasti Ave. 68, Minsk 220072, Belarus
[2] LaserLab ELETTRA-Sincrotrone, Strada Statale 14 – km 163,5 in AREA Science Park, 34012 Basovizza, Trieste, Italy
[3] SOLIX Ltd, Partizansky Ave. 77, Minsk 220107, Belarus

Received: 2 July 2006/Revised version: 7 October 2006
Published online: 2 December 2006 •

ABSTRACT Continuous-wave operation of a diode-pumped Nd:YVO_4 laser with self-frequency Raman conversion is demonstrated. The threshold of Raman generation was measured to be 1.3 W of laser diode power. The maximum output power of Stokes radiation at the wavelength of 1177 nm was up to 50 mW at a laser diode pump power of 2.3 W, corresponding to the slope efficiency of 5%. The beam quality M^2 of the Stokes radiation was about 1.4. The fluctuations of the Stokes power were minimised down to 4%.

PACS 42.55.Ye; 42.60.Pk; 42.65.Dr

1 Introduction

The neodymium-doped yttrium ortho-vanadate (Nd:YVO_4) crystal is an excellent medium for stable and effective diode-pumped solid-state lasers, especially in end-pumped configurations. This crystal possesses such advantages as the broad pump absorption band at 808.7 nm (the line width at room temperature is about 2.5 nm FWHM [1]), large pump absorption cross section ($2.7 \times 10^{-19}\,cm^2$ for Nd:YVO_4 crystal and $0.7 \times 10^{-19}\,cm^2$ for Nd:YAG crystal [2]), large stimulated emission cross section ($15 \times 10^{-19}\,cm^2$ at 1064 nm for an *a*-axis cut, being about four times larger than that of Nd:YAG), a higher allowable doping level and anisotropic gain which provides the polarised output. These advantages simplify wavelength tuning and the pump beam collimating requirements for diode pumping. The short upper-state lifetime of Nd:YVO_4 crystal allows faster Q-switching [3], mode-locking operation [4] and simultaneous Q-switching and mode locking [5, 6]. The efficient high-power continuous-wave (cw) laser operation was also demonstrated with the end-pumped Nd:YVO_4 laser [7]. Up to 11 W of output radiation was generated at a diode pump power of 22 W.

YVO_4 crystal is also a perspective medium for stimulated Raman scattering (SRS) [8] with two SRS active vibration modes: $890\,cm^{-1}$ and $815\,cm^{-1}$. Application of Nd:YVO_4 crystal for self-frequency Raman conversion in passively Q-switched microchip lasers with cw diode pumping was first successfully demonstrated in [9]. The Raman gain coefficient of Nd:YVO_4, comparable to or even higher [8, 10] than those of double-tungstate crystals, and short dephasing time (about 3.5 ps) for the 890-cm^{-1} mode provide a relatively high conversion efficiency (3%) of diode laser power to Stokes power and subnanosecond pulse generation at the Stokes wavelength. Later, in similar conditions, the conversion efficiency was increased up to 6.3% [11] due to the use of a more powerful (up to 2 W) pump source. Also, the high-energy self-frequency Raman generation in Nd:$GdVO_4$ crystal (which is similar to Nd:YVO_4 crystal) was successfully demonstrated [12].

In recent years, the possibility of cw generation in lasers with Raman crystals has been attracting great attention [13–17]. Recently, the possibility for cw self-frequency Raman conversion in a Nd:KGW laser with cw diode pumping has been demonstrated for the first time [15]. It was shown that the use of lasers with high-reflective mirrors both at laser and first Stokes wavelengths allows the Raman threshold to be reached even in the cw regime. The cw intracavity Raman conversion was also first demonstrated with $Ba(NO_3)_2$ [16] and $PbWO_4$ [17] crystals placed in a diode-pumped Nd:YVO_4 laser. Later, the cw Raman generation was also obtained in KGW crystal placed in the cavity of a diode-pumped Nd:YAG laser [18].

Compared to Nd:KGW, the Nd:YVO_4 crystal is more applicable for cw self-frequency Raman conversion due to the relatively high thermal conductivity, symmetrical thermal lens and narrow spectral line width of generation typical for this crystal, which are important for obtaining the high spectral brightness favourable for reaching the Raman threshold. In this paper we demonstrate for the first time the cw self-frequency Raman conversion in a Nd:YVO_4 laser with diode pumping.

2 Experimental setup

The optical scheme of the laser with cw self-frequency Raman conversion based on Nd:YVO_4 crystal is presented in Fig. 1. A fibre-coupled (100 μm) laser diode (2.4 W at 0.8075 mm, model ML151 from Milon Laser) con-

✉ Fax: +375-17-284-16-65, E-mail: lva76@yahoo.com

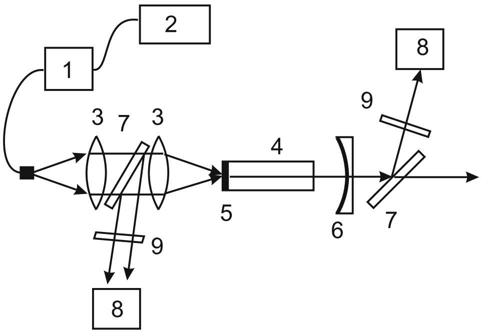

FIGURE 1 Experimental scheme of diode-pumped laser with self-frequency Raman conversion on the base of Nd:YVO_4 crystal. 1 – diode laser; 2 – driver; 3 – lenses; 4 – active element; 5 – input mirror; 6 – output coupler; 7 – beam splitters; 8 – power meters; 9 – interference filters

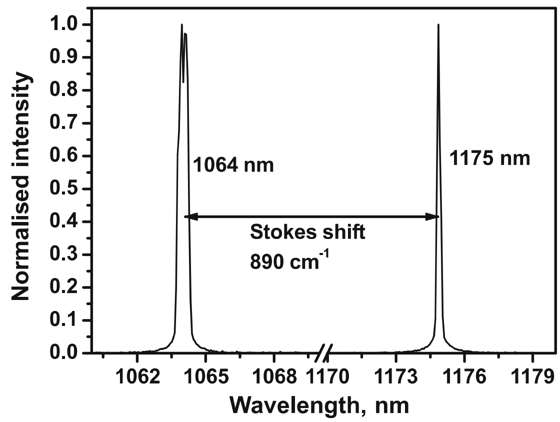

FIGURE 2 Emission spectrum of diode-pumped Nd:YVO_4 laser at fundamental and Stokes wavelengths for maximum pump power

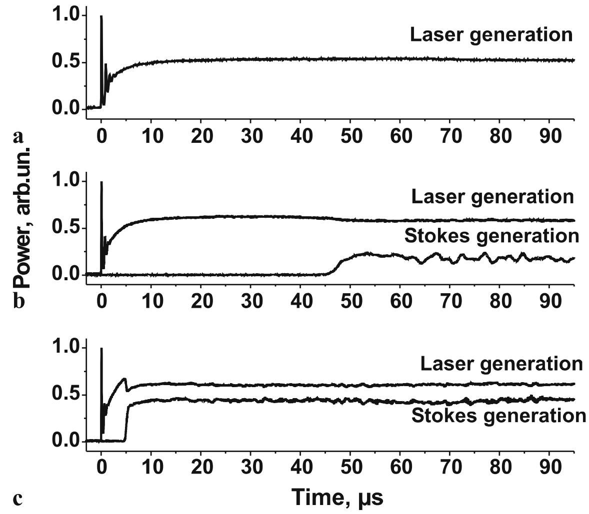

FIGURE 3 Oscilloscope traces for laser and Stokes evolution for different pump powers: (**a**) 0.8 W, (**b**) 1.4 W, (**c**) 2.3 W

nected to the laser driver (model LDD-10 from ATC SD, Russia) was used for a pump source. The beam exiting the fibre was imaged onto the laser crystal by a two-lens coupling system installed in front of the optical fibre, providing a nearly Gaussian intensity profile with a diameter of 100 μm ($M^2 = 42$).

The laser comprised an active element placed between two mirrors. The active element was a Nd(0.8 at. %):YVO_4 (*a*-cut) crystal with the length of 22 mm. The crystal was mounted on a copper heat sink with use of heat-conducting paste. The flat input mirror was coated on a pumpable facet of the active element. This mirror had a reflectance of 99.6% and 99.94% at 1064-nm and 1175-nm wavelengths, respectively, and a transmittance of 97.5% at the pump wavelength. The other facet of the active crystal had an antireflective coating for a spectral range of 1060–1200 nm ($R < 0.1\%$). The output spherical coupler with a radius of curvature of 46 mm had a reflectance of 99.95% at the laser wavelength of 1064 nm and 99.85% at the 1175-nm wavelength. The geometrical length of the cavity was about 50 mm. The output power at fundamental and Stokes wavelengths was measured at both sides of the laser cavity. For this purpose the beam splitters were used. They directed some part of the generated radiation to power meters. To separate laser and Stokes radiation, the interference filters were used.

3 Results and discussion

The generation threshold at the fundamental wavelength of the Nd:YVO_4 laser was reached at a pump power of ~ 0.05 W of the laser diode power. The laser cavity mirrors used in the experiments provide a lower threshold. The relatively high threshold obtained can be explained by the low quality of the laser crystal. The lowest Raman threshold established in the experiments was nearly 1.3 W of the pump power. Figure 2 presents the spectrum of the Nd:YVO_4 laser output with the laser and Stokes lines. The Stokes line was observed at 1175 nm with a shift of 890 cm^{-1} towards the fundamental laser line at 1064 nm. No more Stokes lines were observed in the experiments. The line widths (FWHM) of the laser and Stokes wavelengths were 4.5 and 1.2 cm^{-1}, respectively. No noticeable line broadening or structure formation in the Stokes spectrum was observed with increasing pump power up to the maximum available level.

Typical oscilloscope traces at the start of laser and Raman generation are presented in Fig. 3. Figure 3a shows the start of laser generation at the pump power when no Stokes generation occurs. The relaxation oscillations related to the initiation of laser generation and continuous transition to the steady-state level are observable. The duration of these oscillations reduces when the pump power increases (Fig. 3b and c). The oscilloscope traces for laser and Stokes radiation not far and far from the Raman threshold are presented in Fig. 3b and c, respectively. The significant (more than 40 μs) delay of the Stokes rise edge relative to the moment when the laser power reaches the level needed for attaining the Raman threshold is seen (Fig. 3b). This delay is the specific behaviour of SRS in the cw regime [15] that corresponds to the evolution of Stokes radiation from the noise level to the steady-state level. Because the single-pass gain of Stokes radiation is small with cw Raman lasers, the Stokes photons are accumulated in the laser cavity slowly, and therefore the time needed for the development of Stokes radiation can be substantial. The higher the laser power and, as a consequence, the higher the gain of Stokes radiation, the shorter the time for Stokes radiation buildup (Fig. 3c).

The dependence of the time for Stokes radiation buildup (T_B) on the laser power can be expressed as [15]

$$T_B = 25\frac{L_C}{c}\frac{1}{G_S P_P - L_S}, \tag{1}$$

where P_P – intracavity power at laser wavelength, L_C – optical length of laser cavity, c – light velocity, G_S – single-pass gain of Stokes radiation per unit pump power and L_S – single-pass losses of Stokes radiation. The experimentally measured dependence of delay time T_B on pump power and its approximation with expression (1) is presented in Fig. 4. The good fitting between the experimental and calculated curves can be observed. The approximation with expression (1) allows estimation of the value $L_S\,(25L_C/c)^{-1}$. Taking into account the optical length of the laser cavity (7.2 cm), the single-pass losses of Stokes radiation (L_S) were calculated to be about 0.7%–1%.

Figure 3 also shows that there are significant fluctuations in Stokes radiation near the Raman threshold compared to those in laser radiation (Fig. 3a and b). The increase in the pump power leads to the stabilisation of Stokes radiation (Fig. 3c). The dependences of standard deviation (σ) normalised to the mean value of laser and Stokes radiation on the pump power are plotted in Fig. 5. It can be seen that the fluctuations for Stokes radiation at the Raman threshold are significantly larger than those for laser radiation. This behaviour was observed for SRS at a nanosecond multimode pulse pump [19] and can be explained by the dramatic effect of power fluctuations for multimode radiation at the fundamental wavelength in the threshold condition. This effect was also demonstrated for cw Raman generation with external multimode pumping [13, 14]. At higher pump power, the strong stabilisation of the Stokes power occurs. The normalised standard deviation of Stokes radiation decreases from 40% to 4%, which is very close to the standard deviation of fundamental radiation (2.8%).

The fundamental and Stokes beams had a smooth, nearly Gaussian spatial intensity distribution. The Stokes beam quality factor M^2 did not exceed 1.4. Figure 6 gives the total output power from the two mirrors at fundamental and Stokes wavelengths as a function of the laser diode power. The maximum Stokes total power was measured as 53 mW at the incident diode power of 2.3 W, corresponding to a slope efficiency of about 5%. The dependence of the conversion efficiency of laser diode power to Stokes power is also plotted in Fig. 6. It can be seen that the conversion efficiency reached 2.2%. The maximum intracavity laser power and intensity were estimated as 11 W and 49 kW/cm^2, respectively. The Stokes intracavity power and intensity were 25 W and 106 kW/cm^2, respectively. It is evident from Fig. 6 that with the reached Raman threshold, the growth of laser intensity slows down slightly. This behaviour was also observed in a previous work [17] and is due to the strong conversion of laser power to Stokes power. Basically, at the Raman threshold, the laser power in the cavity should be equal to that of the Raman threshold and, actually, should not increase any more [20]. The increase in the laser power after the Raman threshold which we observed in our experiment can be explained by the wider spectral bandwidth of laser radiation compared to that of Stokes radiation.

The Stokes generation efficiency and power can be increased by optimising the cavity parameters, decreasing the laser fundamental line width to the line-width value of spontaneous Raman scattering for YVO_4 crystal and by utilising a longer Raman Nd:YVO_4 crystal of better quality. Our estimations show that the two times increase in the active Raman crystal length leads to nearly the two times decrease in the Ra-

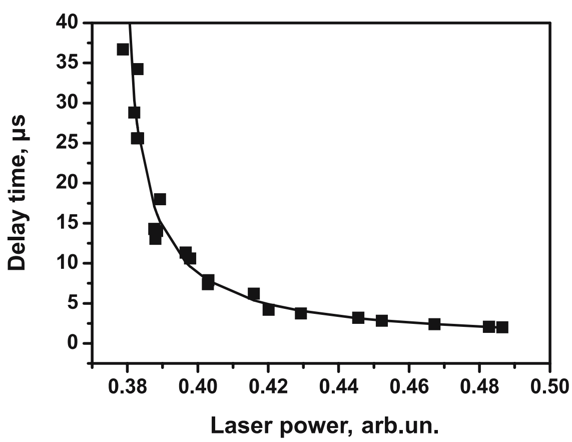

FIGURE 4 The dependence of delay time for the Raman signal on the average power of laser radiation. *Squares* – experimental data, *curve* – their approximation with expression (1)

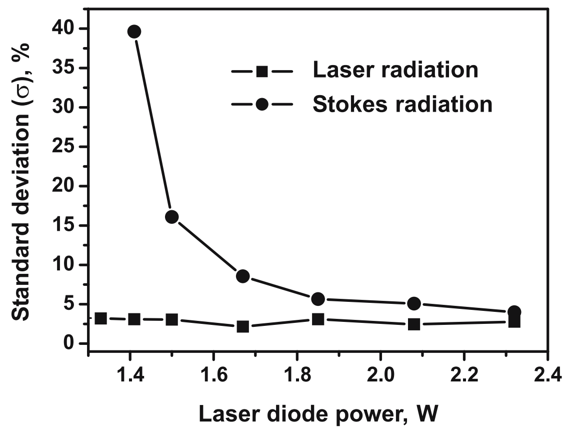

FIGURE 5 The dependences of normalised standard deviation for laser and Stokes powers on laser diode power

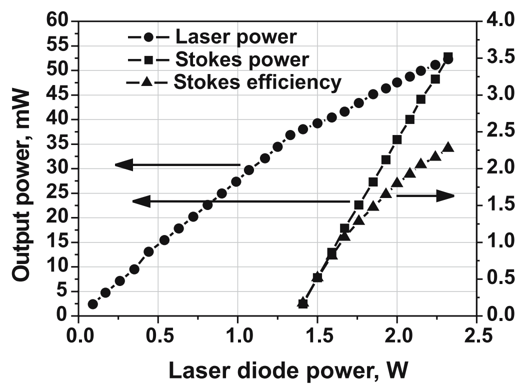

FIGURE 6 The dependences for powers of laser and Stokes radiation and for conversion efficiency on laser diode power

man threshold power and correspondingly to the increase in the Stokes power up to 90 mW and the generation efficiency from 2.2% up to 4.9% at the specified value of laser diode power.

4 Conclusion

In conclusion, continuous-wave operation of a diode-pumped Nd:YVO_4 laser with self-frequency Raman conversion is reported for the first time. The Raman threshold was measured at 1.3 W of the laser diode power. The highest output power obtained at the Stokes wavelength was 53 mW for a slope efficiency of 5%. The temporal behaviour of the generated Stokes radiation was studied. The analysis of the obtained results shows that Nd:YVO_4 can be a very perspective material for creation of efficient and powerful cw self-Raman lasers if the laser cavity parameters are optimised by increasing the laser crystal length, decreasing the losses at laser and Stokes frequencies and increasing the laser diode power.

ACKNOWLEDGEMENTS The authors thank Prof. W. Kiefer of Würzburg University (Germany) and Prof. P.A. Apanasevich of B.I. Stepanov Institute of Physics (Belarus) for useful discussions of the results.

REFERENCES

1 A.D. Lieto, P. Minguzzi, A. Pirastu, V. Magni, IEEE J. Quantum Electron. **QE-39**, 903 (2003)
2 D.G. Matthews, J.R. Boon, R.S. Boon, R.S. Conroy, B.D. Sinclair, J. Mod. Opt. **43**, 1079 (1996)
3 A. Agnesi, C. Pennacchio, G.C. Reali, Opt. Lett. **22**, 1645 (1997)
4 V. Couderc, F. Louradour, A. Barthelemy, Opt. Commun. **166**, 103 (1999)
5 T.M. Jeong, C.M. Chung, H.S. Kim, C.H. Nam, C.J. Kim, Electron. Lett. **36**, 633 (2000)
6 Y.F. Chen, S.W. Tsai, S.C. Wang, Opt. Lett. **25**, 1442 (2000)
7 Z. Xiong, Z.G. Li, N. Moore, W.L. Huang, G.C. Lim, IEEE J. Quantum Electron. **QE-39**, 979 (2003)
8 A.A. Kaminskii, K. Ueda, H.J. Eichler, Y. Kuwano, H. Kouta, S.N. Bagaev, T.H. Chyba, J.C. Barnes, G.M. Gad, T. Murai, J. Lu, Opt. Commun. **194**, 201 (2001)
9 A.A. Demidovich, L.E. Batay, A.S. Grabtchikov, V.A. Lisinetskii, V.A. Orlovich, A.N. Kuzmin, in *Advanced Solid State Photonics*, ed. by G. Quarles (Optical Society of America, Washington, DC, 2004), p. 304
10 P.G. Zverev, A.Y. Karasik, A.A. Sobol, D.S. Chunaev, A.I. Zagumennyi, Y.D. Zavartsev, S.A. Kutovoi, V.V. Osiko, I.A. Shcherbakov, in *Proc. Advanced Solid State Photonics Conf.*, Santa Fe, New Mexico, 1–4 February 2004 (OSA Tech. Dig.) (Optical Society of America, Washington, DC, 2004), paper TuB10-1
11 Y.F. Chen, Opt. Lett. **29**, 1251 (2004)
12 T.T. Basiev, S.V. Vassiliev, V.A. Konjushkin, V.V. Osiko, A.I. Zagumennyi, Y.D. Zavartsev, S.A. Kutovoi, I.A. Shcherbakov, Laser Phys. Lett. **1**, 237 (2004)
13 A.S. Grabtchikov, V.A. Lisinetskii, V.A. Orlovich, M. Schmitt, R. Maksimenka, W. Kiefer, Opt. Lett. **29**, 2524 (2004)
14 V.A. Lisinetskii, A.S. Grabtchikov, P.A. Apanasevich, M. Shmitt, B. Kuschner, S. Shluecker, V.A. Orlovich, J. Raman Spectrosc. **37**, 421 (2006)
15 A.A. Demidovich, A.S. Grabtchikov, V.A. Lisinetskii, V.N. Burakevich, V.A. Orlovich, W. Kiefer, Opt. Lett. **30**, 1701 (2005)
16 V.A. Orlovich, A.S. Grabtchikov, V.A. Lisinetskii, V.N. Burakevich, A.A. Demidovich, M. Schmitt, W. Kiefer, in *Advanced Solid-State Photonics 2005 Tech. Dig. CD-ROM* (Optical Society of America, Washington, DC, 2005), paper WA6
17 V.A. Orlovich, V.N. Burakevich, A.S. Grabtchikov, V.A. Lisinetskii, A.A. Demidovich, H.J. Eichler, P.Y. Turpin, Laser Phys. Lett. **3**, 71 (2005)
18 H.M. Pask, Opt. Lett. **30**, 2454 (2005)
19 A.S. Grabtchikov, A.I. Vodtchits, V.A. Orlovich, Phys. Rev. A **56**, 1666 (1997)
20 K.S. Repasky, L. Meng, J.K. Brasseur, J.L. Carlsten, R.C. Swanson, J. Opt. Soc. Am. B **16**, 717 (1999)